Multiwavelength Raman Spectroscopy for the Evaluation of Lime Saturation in Cement Raw Mix as a Function of Clay Content

Espectroscopia Raman multilongitud de onda para la evaluación de la saturación de cal en la mezcla cruda de cemento en función del contenido de arcilla

Iliana Rosales-Candelas[1*], David Quiroz-Portillo[2], Juan J. Soto-Bernal[1], Rosario González-Mota[3], Ahiza Martínez-Romo[1], Claudio Frausto-Reyes[4]

(1) Laboratorio de Optoelectrónica, Ingeniería Eléctrica y Electrónica, TecNM/Instituto tecnológico de Aguascalientes, Av. A. López Mateos 1801 Ote. Fracc. Bona Gens, Aguascalientes, Ags., México. C.P. 20256.
(2) Laboratorio de Optoelectrónica, Mantenimiento Electrónico, Cruz Azul Aguascalientes, Carretera Carboneras-Arroyo Hondo km 4. Arroyo Hondo, Tepezalá, Ags., México. C.P. 20657.
(3) Laboratorio de Optoelectrónica, Ingeniería Química, TecNM/Instituto tecnológico de Aguascalientes, Av. A. López Mateos 1801 Ote. Fracc. Bona Gens, Aguascalientes, Ags., México. C.P. 20256.
(4) Laboratorio de Espectroscopia, Centro de Investigaciones en Óptica A.C., Unidad Aguascalientes, Prol. Constitución 607, Fracc. Reserva Loma Bonita, Aguascalientes, Ags., México, C.P. 20200.
*autor de correspondencia (iliana.rc@aguascalientes.tecnm.mx)

ABSTRACT

In this work we analyze the lime saturation module for different clay settings of raw material after raw grinding process by means of a multiwavelength Raman spectroscopy study, at excitation wavelengths of 450, 532, 633 and 780 nm. The data reveal that independently of the wavelength used, the results of the Raman shifts can be used to calculate the setpoint for controlling the alumina in the raw mix that needs to be adjusted to have the lime saturation within quality parameters, with a minimum variation compared with other techniques such as XRF and XRD, thus ensuring that the Clinker phases are formed under quality standards. The intensity ratios of Raman spectra were used to calculate LS values which were close to those obtained with the XRF technique. Therefore, this measurement approach can be used successfully as an effective and alternative non-destructive method to determine the LS of cement raw mix.

Keywords: clay, lime saturation, cement raw mix, Raman spectroscopy, Raman spectra

RESUMEN

En este trabajo se analiza el módulo de saturación de cal para diferentes configuraciones de arcilla mediante espectroscopía Raman a longitudes de onda de excitación de 450, 532, 633 y 780 nm. Los resultados Raman permiten calcular el punto de ajuste para controlar la alúmina en la mezcla cruda, independientemente de la longitud de onda utilizada, esta debe ajustarse para mantener la saturación de cal dentro de los parámetros de calidad, con una variación mínima en comparación con otras técnicas como XRF y XRD, asegurando así, que las fases de clínker se formen bajo estándares de calidad. Las relaciones de intensidad de los espectros Raman se usaron para calcular valores de LS cercanos a los obtenidos con la técnica XRF. Por lo tanto, este método de medición puede utilizarse con éxito como un método alternativo no destructivo eficaz para determinar el LS de la mezcla cruda de cemento.

Palabras clave: arcilla, saturación de cal, mezcla de cemento crudo, espectroscopia Raman, espectros Raman

INTRODUCTION

In the cement industry, Clinker and Portland cement quality depends on raw materials and raw mix which can have a negative influence in the early strength development in cement due to a bad mix design (Taylor, 1997; Duda, 1985, Orazimbetova *et al*., 2023). The raw mix design consists mainly of limestone and clay components which are rich in calcium, aluminum, silicon and iron, which are present as calcium oxide (CaO), aluminum oxide (Al_2O_3), silicon dioxide (SiO_2) and ferric oxide (Fe_2O_3) (Hewlett, 2004). The primary raw material is limestone as a contributor of calcium oxide which is the main oxide of the raw mix. Clay is the secondary component, which contains aluminum oxide, silicon dioxide and ferric oxide. However, if any of these oxides were not found in the limestone or in the clay, it is necessary to get them using other materials called correctors to compensate for lack quantities of such elements Hewlett, 2004). There are chemical relationships to monitor and characterize the raw mix known as modules, these are lime saturation factor (LS), silicon module and alumina module (Fernandez Paris, 1967). For the calculation of these modules the oxide percentages are used which can be determined by chemical analysis. The module for lime saturation is used to set the optimal lime content, the silicon module is related to the rotary kiln temperature at which Clinkerization will take place, and the alumina module characterizes the molten phase composition inside the rotary kiln that can improve the burnability of raw meal and the formation of more alite particles (Zhang *et al*., 2022). The LS can be calculated by Equation 1:

$$LS = CaO * 100/(2.8\,SiO2 + 1.15\,Al2O3 + 0.35\,Fe2O3) \tag{1}$$

Equation 1 indicates the current lime quantity existing in the raw expressed as a percent of the maximum amount of lime that under certain technical conditions of calcination and cooling can be combined with hydraulic factors SiO_2, Al_2O_3, and Fe_2O_3 to form the Clinker phases such as the tricalcium silicate C_3S, dicalcium silicate C_2S, tricalcium aluminate C_3A and tetracalciumferroaluminate C_4AF, which are rich in lime and have the most favorable properties, particularly with regard to the development of cement strengths (Li *et al*; 2024). If there were an excess of uncombined lime in Clinker, this could damage mortars or concrete due to expansion phenomena, by subsequent reaction of the cement with the water. In Clinker, the LS can vary between 92 and 102%. It has been proven that making changes in the amount of oxides, affects the formation of C_3S (Fernández Paris, 1967), being the most important mineral in Clinker and once hydrated, during the hydration process of Portland cement, the calcium silicate hydrate (C-S-H) is produced, which presents a structure in the form of finite chains of tetrahedral silicon with undefined stoichiometry and contributes to the early strength development in Portland cement (Fernández Paris, 1967). The most used techniques to calculate LS of raw material are X-rays (diffraction and fluorescence) and prompt gamma neutron activation analysis, among others (Vázquez, 1980; Bond *et al*., 2000; Fan *et al*; 2020).

In recent years, Raman spectroscopy has gained increasing attention as a powerful analytical tool for the characterization of cementitious materials due to its high spatial resolution and ability to identify mineral phases and chemical bonds in heterogeneous systems. Recent advances have demonstrated that Raman spectroscopy can be effectively applied to investigate clinker composition, monitor hydration processes, and characterize cement microstructures at different spatial scales (Zhang *et al*., 2025). However, Raman spectroscopy, in our knowledge, has not been reported as an analytical method for the study of the lime saturation due to changes in the clay content in a raw mix. The Raman spectroscopy technique was used in this work as an effective and alternative method to determine the lime saturation, because qualitative and quantitative analysis can be carried out and also is useful for material characterization, proving to be a non-destructive analytical tool capable of obtaining vibrational, rotational and other low-frequency modes of the selected target (Ruchita & Agrawal, 2011).

Raman spectra of materials such as clay minerals were unavailable until powerful laser spectrometers became accessible. In this way, Raman shifts have already been reported for limestone, clay, and hematite where laser sources of excitation in the near ultraviolet, visible, or near-infrared range have been used for the analysis (Borromeo *et al*., 2018; Lalla *et al*., 2015; Cuéllar *et al*., 2010; Kloprogge, 2017). Recent spectroscopic studies have provided detailed vibrational characterization of clinker phases using Raman and infrared techniques. For

instance, Król *et al*. (2022) reported comprehensive assignments of vibrational bands for major clinker minerals such as C3S, C2S, C3A and C4AF, demonstrating the capability of Raman spectroscopy to accurately identify cement mineral phases and their spatial distribution within clinker samples.There are different techniques for quantification through Raman spectroscopy, such as the proportional relationship between Raman scattering intensity and analyte concentration.Furthermore, recent developments in Raman imaging techniques have enabled detailed phase-specific characterization of clinker particles. Polavaram & Garg (2023), demonstrated that Raman imaging can be used to determine particle size distribution and morphological characteristics of individual clinker phases, highlighting the potential of Raman-based techniques for advanced analysis of cement systems.The quantitative analysis can be done using changes in Raman band position or band shape (Pelletier, 2003). As a result of the quantitative analysis of the Raman scattering intensity, the particular data acquired from each spectrum of raw mix can be used to calculate the intensity ratio of a determined Raman shift band for different clay content to decide the amount of clay that is needed to improve the raw material quality. It is worth mentioning that with the current method using X-ray fluorescence radiation, the adjustment of the raw mixture is carried out empirically by the operator. Confocal Raman microscopy has also been successfully applied for in-situ characterization of hydration processes in modern cement systems. Recent studies have shown that Raman spectroscopy can monitor the formation of hydration products such as portlandite, ettringite and carboaluminates in limestone calcined clay cements, providing valuable information about reaction mechanisms and phase evolution (Mañosa *et al*., 2024).

With the method proposed by Raman spectroscopy, it is through the calculation of the intensity's ratios of the Raman bands. In addition, a portable Raman device can be used to perform measurements on the raw mixture in the field optimizing the speed of adjustment in the concentration of the oxides. In addition, recent studies have explored rapid spectroscopic approaches for the quantitative determination of oxide composition in cement raw meals. For example, Ma *et al*. (2025), demonstrated that the fusion of laser-induced breakdown spectroscopy and near-infrared spectroscopy significantly improves the quantitative prediction of CaO, Al_2O_3, Fe_2O_3 and SiO_2 concentrations in raw materials used in cement production. These developments highlight the growing interest in spectroscopic techniques capable of providing faster compositional analysis compared with conventional laboratory methods. With this approach, in this work it has been confirmed that changes in the oxide concentration of cement raw materials can be detected after adjusting the clay component in the Polab system and the LS module can be calculated and corroborated according to the Raman spectra.

MATERIALS AND METHODS

For the development of this work, raw materials for raw mixing, such as limestone and clay were used as main contributors of calcium, alumina and silica; hematite was used as a material corrector of ferric oxide; and fluorite was used as a flux corrector and mineralizer inside the rotary kiln. These raw materials are impure as they may contain other elements such as quartz and magnesium oxide among others. However, the control of such elements is outside the scope of this work. Only the content of clay component was modified in the raw mix. Raw material samples were prepared in a Polab system after a raw grinding process (13 samples). The raw mix sample arrives at the laboratory by means of a pneumatic system; then it is ground in a small mill for 150 seconds and then pressed to form the sample to be analyzed. The sample size is 5 cm in diameter. The chemical analysis of the samples was obtained by X-ray fluorescence spectrometry (XRF, Zetium). Raman spectra were acquired with a Thermo Scientific DXR Spectrometer with spatial resolution of 3 μm, pinhole aperture 50 μm, grating 400 lines/mm, allowed range of 3400 to 200 cm^{-1}. All the spectra were obtained with a Mplan 50 x/.75 objective. Laser sources of excitation at different wavelengths were used, which were 455, 532, 633, and 780 nm at a power of 5 mW on the surface of the samples. All acquisitions were carried out with dispersive Raman software. Same raw mix samples were used for analysis in the XRF as well as for performing the measurements in the Raman microscope.

To characterize clay adjustment, percentages of 2.80, 2.90, 3.20, and 3.40 were used in a Polab system, these adjustments were taken as a consequence of the results of the previous chemical analysis, owing to the raw material conditions and calcination process. The setting range for clay component is 3 to 5%, which is fixed by each cement plant. With this range of values, it is expected to approach the LS to 100%, ensuring that the raw

mixture is within quality parameters to form Clinker. Nevertheless, the limestone used in the raw mixture comes from different benches or deposits which could affect the raw mixture; thereby the analysis of limestone is beyond the scope of this work. Clay adjustments were carried out in two parts. First it varied to 3.20 and 3.40%, and one month later to 2.80 and 2.90%. For (clay content) of 3.20% the value of LS was 102%, which indicates an excess of lime in the mixture. Because of this, another adjustment of 3.40% clay setting was made, resulting in LS of 101.5%. With this last value of LS, the lime excess was reduced. To corroborate the effect in LS when adjusting clay the following setting was made; for an adjustment of 2.90% the value of LS was 101.6%, the new setting is to decrease the amount of clay from 2.90% to 2.80% resulting in LS equal to 102.1%. These settings are normally made empirically, which might cause variations in the LS and consequently have no control in the raw mixture. With Raman spectroscopy it is intended to have more efficient raw mix control and be able to select the clay percentage that leads to a LS value within accepted specifications.

RESULTS AND DISCUSSION

XRF

After each adjustment in the clay component the raw mixture samples were analyzed in the XRF, where the chemical analysis of raw mix was realized according to clay adjustments. The analysis from 3.20 to 3.40% is shown in Table 1. It is worth mentioning that only the main oxides are shown.

When varying the clay setting, the percentage of oxides and therefore the LS value vary; accordingly, however, values of 100% have not been reached, which requires further adjustments, which could be a long process due to the raw mix. Table 2 shows values of LS and oxides, after adjusting the clay from 2.80 to 2.90%.

Table 1: Chemical analysis of raw mixture in accordance with clay setting and LS from 3.20 to 3.40%.

Oxides %	Clay setting %	
	3.2	3.4
CaO	44	43.99
SiO_2	13.51	13.54
Al_2O_3	3.17	3.18
Fe_2O_3	2.32	2.34
LS %	102.2	101.5

Table 2: Chemical analysis of raw mixture in accordance with clay setting and LS from 2.80 to 2.90%.

Oxides %	Clay setting %	
	2.8	2.9
CaO	44.05	44.06
SiO_2	13.73	13.77
Al_2O_3	3.2	3.32
Fe_2O_3	2.26	2.27
LS %	102.1	101.6

As mentioned earlier, the clay adjustments from 2.90 to 2.80% and 3.20 to 3.40% were made at different dates. Therefore, their results have no relationship between them. It is worth mentioning that these results are obtained by means of the control system Polab.

As shown in Table 1 and 2, the chemical composition of the samples of raw mixture contains CaO, Fe_2O_3, Al_2O_3, and SiO_2, which are the main oxides. CaO and SiO_2 were not detected in the Raman spectra, however Al_2O_3, Fe_2O_3 and $CaCO_3$ bands were registered. A multiwavelength Raman spectroscopy was used to study the changes in the concentration of Al_2O_3, Fe_2O_3 and $CaCO_3$ oxides in the raw mixture after each adjustment in the clay component, to corroborate if there is a correlation with the results obtained with the fluorescence X-ray technique. $CaCO_3$ and Al_2O_3 were detected at the region of 708-1086 cm^{-1} (these two bands can be attributed to both oxides), $CaCO_3$ and Fe_2O_3 at the Raman shift of 279 cm^{-1}, these bands have already been reported (Borromeo *et al*., 2018; Lalla *et al*., 2015; Cuéllar *et al*., 2010; Kloprogge, 2017). Recent spectroscopic investigations have further confirmed the capability of Raman spectroscopy to identify clinker-related mineral phases and carbonate components in cement systems, providing reliable vibrational fingerprints for materials such as calcite, hematite and alumina-bearing phases (Król *et al*., 2022; Zhang *et al*., 2025).

It should be noted that the strongest peaks are not only due to a higher concentration of the substance but also for a strong molecular vibration. Independently of the wavelength used, according to the multiwavelength analysis, the Raman shifts are always the same. Changes in the concentration of oxides can be observed in the Raman spectra shown in Figure 1 at an excitation wavelength of 780 nm after clay adjustments of 2.80, 2.90, 3.20, and 3.40% for raw mix. It is noteworthy that fluorescence is absent, allowing calculating the intensity ratios of the Raman peaks which indicate the changes of the component concentration.
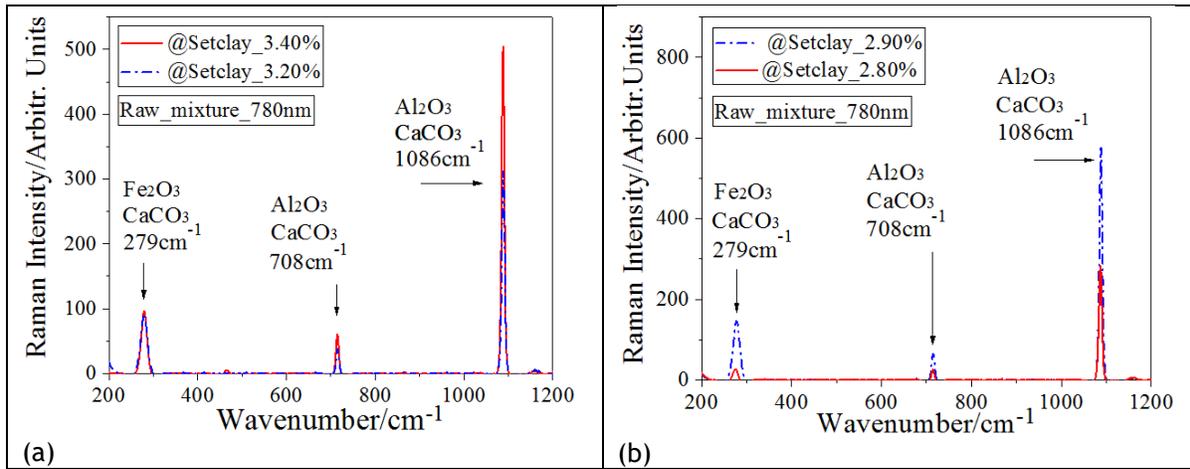

Fig. 1: Raman spectra at excitation wavelength of 780 nm of raw mix for different clay settings, (a) 3.20, 3.40, (b) 2.90, 2.80.

To corroborate the Raman shifts detected in the Raman spectra from the raw mix, several samples of pure hematite and limestone were analyzed, corresponding to Fe_2O_3 and $CaCO_3$ and the same bands have been found. As seen in Figure 2, Raman peaks at 279, 708 and 1086 cm^{-1} were particularly labeled to emphasize the same peaks observed in Figure 1 for the oxides mentioned. The Raman spectrum of hematite from Figure 2 (a) reveals that the peak intensity of the Raman shift of 279 cm^{-1} is more intense than the recorded in the raw mix spectra from Figure 1, this is because the percentage of hematite in the raw mix is about 1 %. Likewise, the Raman spectrum of limestone that is shown in Figure 2 (b) was obtained only to validate the Raman shifts of 279, 708 and 1086 cm^{-1} that correspond to $CaCO_3$, obtained in the Raman spectra of the raw mix.
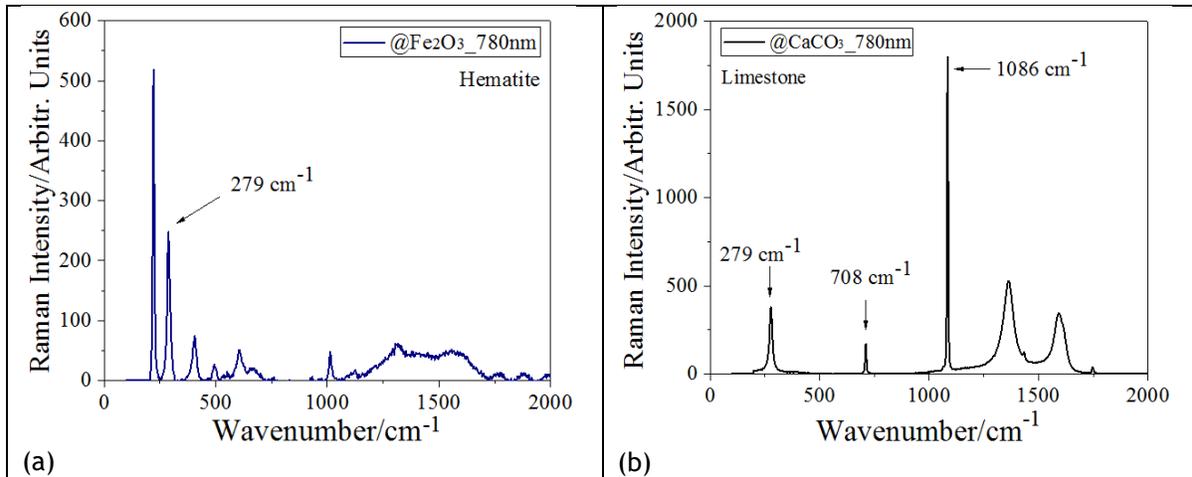
Fig. 2: Raman spectra at an excitation wavelength of 780 nm, (a) hematite (Fe_2O_3), (b) limestone ($CaCO_3$).

Calculated intensity ratios and lime saturation

Changes in the concentration of oxides in the raw mix sample after clay settings can be observed in the Raman spectra by means of changes in the intensities of the peaks of the Raman shifts. The calculation of intensity ratios can be used to indicate the amount of clay that is necessary to adjust in the Polab system to get LS values that allow forming clinker. Aluminum oxide is one of the main clay components and thus its characteristic Raman bands were used in calculations. Even though the same bands may also be attributed to limestone, they act as a probe for the amount of oxide content in the raw mix, and our particular interest is focused on the aluminum oxide. The intensity ratios were calculated for each clay adjustment, (1) 3.20% to 3.40% and (2) 2.90% to 2.80%, at different excitation wavelengths (455, 532, 633 and 780 nm) considering the intensity of the Raman peaks, for each recorded band between clay adjustments. The procedure was carried out as follows: first the intensity ratio for 708 cm^{-1} (R_{708}), then the ratio for 1086 cm^{-1} (R_{1086}), and finally adding both ratios $R_{sum} = R_{708}$ + R_{1086}, where R_{sum} is the setpoint for controlling the alumina in the raw mix through the clay component. The ratios were obtained dividing the higher intensity (HP) by the lower intensity (LP) for each band (HP/LP). For both clay adjustments the Raman spectra reveal changes in the concentration of oxides as shown in Figure 1. For clay settings from 3.20 to 3.40%, there was an increase in the peak intensity of Raman shifts, thus for 3.40% the value for HP was taken, whereas for clay settings from 2.90 to 2.80%, the Raman spectra reveal a decrement in the peak intensities, therefore HP was taken for 2.90%. The calculated ratios at different sources of excitation for each Raman shift are listed in Table 3 for clay setting from 3.20 to 3.40% where variations in some of the ratios can be observed if one compares the values obtained for different Raman shifts. This could be due to the heterogeneity of the sample owing to impurities in the area where the spectrum was measured. R_{sum} represents the total amount of alumina in the raw mixture and can be used to calculate LS according to equation 1 (i.e. the Al_2O_3 term). The LS values obtained from these calculations are also shown in Table 3.

Table 3: Calculated intensity ratios and LS at different wavelength for clay setting from 3.20 to 3.40%

Wavelength (nm)	R_{708}	R_{1086}	R_{sum}	LS
780	1.59	1.61	3.2	101.8
633	1.61	1.67	3.28	101.5
532	1.54	1.11	2.65	103.3
455	1.97	2.15	4.12	99.3

Similarly, Table 4 shows the intensity ratios and LS calculated for clay settings from 2.90 to 2.80%, at different wavelength, which also reveals that there are variations in the ratios owing possibly to the heterogeneity of the sample.

Table 4: Calculated intensity ratios and LS at different wavelength for clay setting from 2.90 to 2.80%

Wavelength (nm)	R_{708}	R_{1086}	R_{sum}	LS
780	2.57	2	4.6	96.9
633	1.17	1.13	2.3	103.2
532	1.01	1.29	2.3	103.2
455	1.49	1.35	2.84	101.5

The data in Table 3 and 4 were used to obtain the graphs shown in figure 3 and 4, respectively for a better visualization. As can be observed, the ratio values for each band that were calculated at a different excitation wavelength clearly show that the behavior of the system is almost the same; the LS values obtained from the sum of the intensity ratios are close to those calculated by the XRF method, also revealing that a relationship exists between the current method (XRF) and the proposed one by Raman spectroscopy because both methods are based on concentration changes in the oxides present in the raw mix, and thus can be used as complementary methods.

Recent studies have shown that spectroscopic approaches can provide reliable quantitative information for cement raw materials and clinker phases when appropriate spectral features are correlated with oxide concentrations (Polavaram & Garg, 2023; Ma *et al*., 2025). Nevertheless, we are aware that the number of samples is small, and further work is necessary with more samples in order to improve the selection of the best clay settings. Although each cement plant sets its own quality parameters for the LS, Raman spectroscopy can be used to adjust the clay to get LS within the allowed values. Additionally, with this novel method, the LS can be calculated in a fast and reliable way because it can select a clay value without relying on the experience of operators of the quality system.
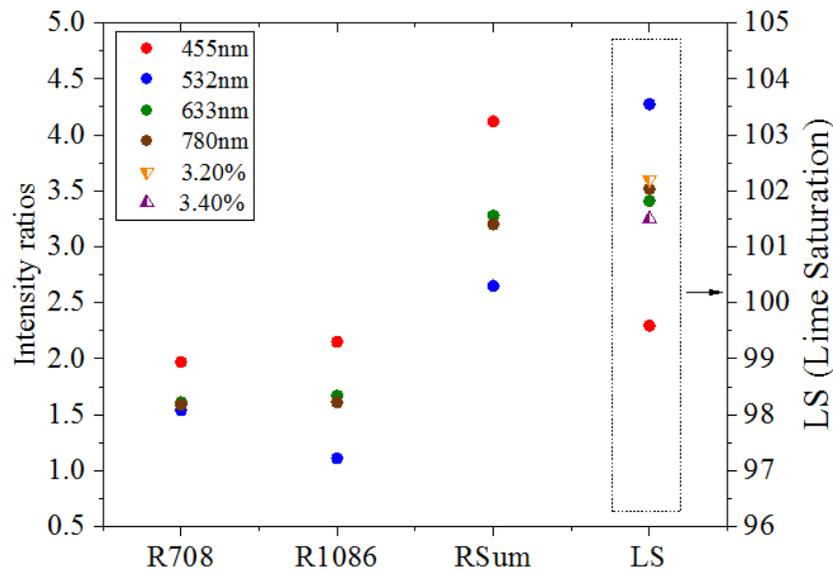

Fig. 3: Intensity ratios and LS for the clay setting from 3.20 to 3.40 % at 455, 532, 633 and 780 nm.
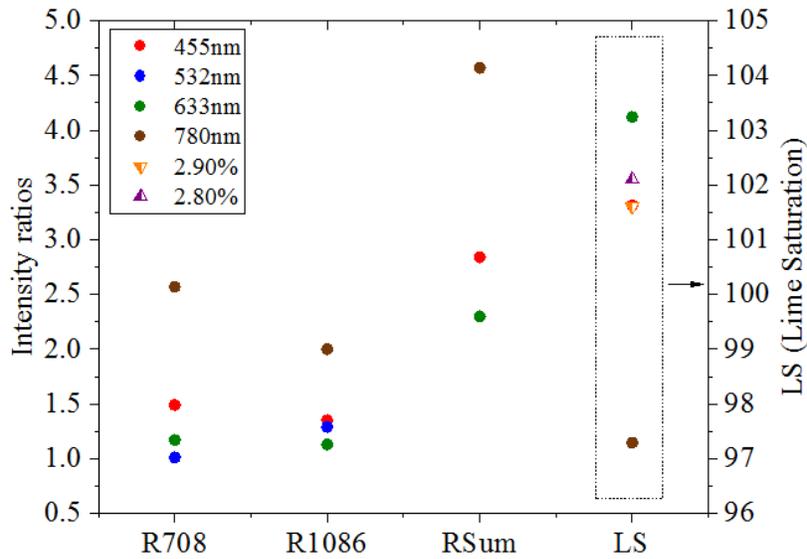
Fig. 4: Intensity ratios and LS for the clay setting from 2.90 to 2.80% at 455, 532, 633 and 780 nm.

Therefore, the multiwavelength analysis performed using Raman spectroscopy demonstrates a reliable and consistent approach for the quantification of the lime saturation module (LS). Similar conclusions regarding the applicability of Raman spectroscopy for monitoring phase composition and reaction products in cementitious materials have been reported in recent studies employing Raman imaging and confocal Raman microscopy (Mañosa et al., 2024; Zhang *et al.*, 2025). An additional advantage of this approach is that the analysis can be performed in situ, without requiring prior preparation of the raw material. In contrast, automated systems currently used in cement plants involve several steps that significantly increase the analysis time. In these systems, the powder sample collected in the field must first be transported through the pneumatic mail system to the laboratory station (Polab), where it undergoes preparation before the analysis is carried out using X-ray techniques. After the measurement, the sample is typically destroyed. By comparison, Raman spectroscopy allows the analysis to be completed within a few minutes without destroying the sample, while simultaneously providing both qualitative and quantitative information about the raw mixture composition.

CONCLUSIONS

Raman spectroscopy was successfully applied to determine the lime saturation module (LS) of cement raw mix with different clay adjustments. The intensity ratios of the Raman bands were used to calculate LS values that were close to those obtained using the XRF technique. These results demonstrate that Raman spectroscopy can be used as an effective and alternative non-destructive method for estimating the LS of cement raw mixtures.

This approach enables the adjustment of clay content to obtain a raw mix with appropriate oxide proportions and LS values within the specifications required by cement plant quality control systems. Furthermore, the LS could be calculated in situ using a portable Raman analyzer combined with an appropriate algorithm, allowing faster analysis compared with conventional methods.

Finally, the results suggest that this optical approach could be extended to the study of clinker systems, since the contributions of the different oxide-related phases may also be detected using Raman spectroscopy.

ACKNOWLEDGMENT

REFERENCES

Bond, J.E., Coursaux, R. & Worthington, R.L. (2000). Blending systems and control technologies for cement raw materials. *IEEE Ind. Appl. Mag., 6* (6), 49–59. https://doi.org/10.1109/2943.877840

Borromeo, L., Egeland, N., Minde, M.W., Zimmermann, U., Ando, S. Madland, M.V., *et al*. (2018). Quick, Easy, and Economic Mineralogical Studies of Flooded Chalk for EOR Experiments Using Raman Spectroscopy. *Minerals, 8* (6), 221. https://doi.org/10.3390/min8060221

Cuéllar, A., Mesa, F.A., Vargas, C. & Perilla, J.E. (2010). Arcillas modificadas caracterizadas por micro-Raman y difracción de rayos X. *Dyna, 77* (164), 39–44.

Duda, W.H. (1985*). Cement data book*, Vol 1, International Process Engineering in the cement industry, third edition. Bauverlag Berlin.

Fan, J., Xu, J. & Wang, Ch. (2020), Overview of Industrial Materials Detection Based on Prompt Gamma Neutron Activation Analysis Technology. *World Journal of Engineering and Technology, 8* (3), 389-404. https://doi.org/10.4236/wjet.2020.83030

Fernandez Paris, J.M. (1967). Dosificación de crudos de cemento Portland mediante el módulo de cal. *Mater. Construcción, 17* (125), 27-46. https://doi.org/10.3989/mc.1967.v17.i125.1665

Hewlett, P.C. (2004). *Lea"s Chemistry of Cement*, fourth ed. Butterworth-Heinemen, Oxford, England.

Kloprogge, J.T. (2017). *Raman Spectroscopies of Clay Minerals*, 1st ed., vol. 8. Elsevier Ltd. pp.150-199. https://doi.org/10.1016/B978-0-08-100355-8.00006-0

Król, M., Koleżyński, A., Florek, P., Jeleń, P., Kozień, D. & Mozgawa, W (2022). Full spectroscopic characterization of clinker minerals (anhydrous cement). *Journal of Molecular Structure, 255*, 132454. https://doi.org/10.1016/j.molstruc.2022.132454

Lalla, E.A., López-Reyes, G., Sansano, A., Sanz-Arranz, A., Schmanke, D., Klingelhöfer, G., *et al*. (2015). Estudio espectroscópico y DRX de afloramientos terrestres volcánicos en la isla de Tenerife como posibles análogos de la geología marciana. *Estudios Geológicos, 71* (2), e035. https://doi.org/10.3989/egeol.41927.354

Mañosa, J., Torres-Carrasco, M., Córdoba, C., Maldonado-Alameda, A. & Chimenos, J.M. (2024). In-situ characterisation of early hydration of low-carbon cements containing thermally and mechanically activated kaolin. *Construction and Building Materials, 457*, 139469. https://doi.org/10.1016/j.conbuildmat.2024.139469

Ma, X., Cai, Y., Wang, X., Zhang, R., Chen, Y. & Huang, B. (2025). Quantitative measurement of cement raw meal composition via spectra fusion of laser-induced breakdown spectroscopy and near-infrared spectroscopy. *Measurement, 253*, Part D, 117865. https://doi.org/10.1016/j.measurement.2025.117865

Orazimbetova, G., Turdialiev, U. & Biniyazova, L. (2023). *Composition of raw mixes for portland cement clinkers using andesic basalt rock*. E3S Web of Conf. Volume 452, 2023. XV International Online Conference "Improving Farming Productivity and Agroecology – Ecosystem Restoration" (IPFA 2023). https://doi.org/10.1051/e3sconf/202345206001

Polavaram, K.C. & Garg, N. (2023). Elucidating the Size and Shape of Individual Clinker Phases via Raman Imaging. *Journal of Physical Chemistry C, 127* (34), 17157–17170. https://doi.org/10.1021/acs.jpcc.3c03453

Pelletier, M.J. (2003). Quantitative Analysis Using Raman Spectrometry. *Appl. Spectroscopy, 57* (1), 20A-42A. https://doi.org/10.1366/000370203321165133

Ruchita, S. & Agrawal, Y.K. (2011). Raman spectroscopy: Recent advancements, techniques and applications. *Vibrational Spectroscopy, 57* (2), 163-176. https://doi.org/10.1016/j.vibspec.2011.08.003

Taylor, H.F.W, (1997). *Cement chemistry*. 2nd ed. Heron Quay London.

Vázquez, T. (1980). Aplicaciones prácticas de la espectroscopía de absorción infrarroja en el estudio de los crudos, del clínker y del cemento portland anhidro. *Mater. Construcción, 30* (179), 101–110. https://doi.org/10.3989/mc.1980.v30.i179.1052

Li, X., Ma, B., Ji, W., Dou, S., Zhou, H., Zhang, H. & Wang, J. (2024). Impact of Lime Saturation Factor on Alite-Ye'Elimite Cement Synthesis and Hydration. *Materials, 17* (12), 3035. https://doi.org/10.3390/ma17123035

Zhang, Z., Huang, Z., Shi, Ch., Wu, Z., Zhang, W., Duan, P, et al. (2025). Advancement in Raman spectroscopy for characterizing cementitious materials. *Journal of the American Ceramic Society, 108,* e20162. https://doi.org/10.1111/jace.20162

Zhang, W., Luan, Z., Ren, X., Ye, J., Shi, D. & Zhang, H. (2022). Influence of alumina modulus on formation of high-magnesium clinker and morphological evolution of MgO. *Cement and Concrete Research, 162*, 106986. 106986. https://doi.org/10.1016/j.cemconres.2022.106986